Phys. Biol. **6** (2009) 025008 (11pp) doi:10.1088/1478-3975/6/2/025008

# The physics behind the larger scale organization of DNA in eukaryotes

**Marc Emanuel, Nima Hamedani Radja, Andreas Henriksson and Helmut Schiessel**

Instituut Lorentz voor de theoretische natuurkunde, Universiteit Leiden, PO Box 9506, NL-2300 RA Leiden, The Netherlands

E-mail: emanuel@lorentz.leidenuniv.nl

Received 12 September 2008, in final form 13 January 2009
Published 1 July 2009
Online at stacks.iop.org/PhysBio/6/025008

**Abstract**
In this paper, we discuss in detail the organization of chromatin during a cell cycle at several levels. We show that current experimental data on large-scale chromatin organization have not yet reached the level of precision to allow for detailed modeling. We speculate in some detail about the possible physics underlying the larger scale chromatin organization.

## 1. Introduction

The human genome contains approximately $6 \times 10^9$ basepairs, two copies of which lead to roughly 2 m of DNA per cell. On scales larger than the helical repeat length, 3.5 nm, the double helix is well described as a wormlike chain with a persistence length of about 50 nm. Disregarding volume interactions, the diameter of the coil in a theta solvent would be around $\sqrt{2 \times 50\ \text{nm} \times 2\ \text{m}} \approx 450\ \mu\text{m}$. This is an order of magnitude larger than the 10 $\mu$m diameter of the nucleus of a typical cell in which the DNA is always confined.

As a first level of organization the eukaryotic DNA is wrapped around protein spools, each a cylindrical wedge of diameter 6 nm and maximal height 6 nm. About 147 basepairs wrap along a left-handed wrapping path of 1, 67 turns around the octamer. These spools are composed of four pairs of histone proteins, named H2A, H2B, H3 and H4. This octamer, together with the DNA wrapped around, is called the nucleosome core particle (NCP). Its structure is known in great detail from high resolution x-ray crystallography [1]. It is noteworthy to mention that the histone proteins that make up the core, although existing with some variations, are remarkably well conserved between eukaryotes. An important feature of the histones is their tails, flexible positively charged extensions. Through modifications, such as acetylation and phosporylation, it is possible to neutralize charges on the tails. These modifications form a way to regulate the organization of the DNA in the nucleus, as we will discuss in the following sections. There are also other modifications, which do not directly influence the spatial distribution of DNA but influence the binding of proteins. We will not consider them in this paper. For a discussion of the energetics and dynamics involved in single nucleosomes, we refer to other reviews [2, 3].

There is one spool for every 160–240 basepairs. This so-called repeat length varies not only over species, but also over cells within one species. The stretches of DNA connecting two neighboring NCPs are called linker DNA. As a result one obtains a bead-on-a-string structure, sometimes referred to as a 10 nm fiber. This structure is, however, only observed *in vitro* at subphysiological salt concentrations. If we nevertheless assume that such a fiber exists in the nucleus with the same stiffness as for naked DNA, then we find a coil diameter of around $\sqrt{50/200} \times 450\ \mu\text{m} \approx 225\ \mu\text{m}$—a value that is still much larger than the diameter of the nucleus.

In most eukaryotes, a fifth histone is thought to bind the two outgoing double strands at each NCP resulting in a denser structure. From EM measurements, it is concluded that the linker histone assembles the two outgoing strands in a stem 3 nm long [4]. This linker histone has a couple of variants (named H1 and H5), but is also very well conserved. The fact that all the histone proteins are so well conserved through evolution indicates that their functional properties are rather intricate. In the presence of linker histones and for physiological salt concentrations one observes dense fibers, usually referred to as 30 nm or chromatin fibers, that have been known through *in vitro* experiments for over 30 years. They typically feature around 30 nm diameter, independent of whether they are extracted from cells or whether they are reassembled. These fibers have a contour length that is only about 1/50th of the contour length of the DNA that it contains but seem to be much stiffer than the naked DNA. Assuming a fiber persistence length of 240 nm [5] leads to a coil size of

 

$\sqrt{2 \times 240\ \text{nm} \times 2\ \text{m}/50} \approx 140\ \mu\text{m}$. If these stiff chromatin fibers really exist *in vivo*, this would call for another level of organization/condensation before the genetic material fits into the nucleus. This larger scale organization will be the main issue we will address in this paper.

Our paper is organized as follows. In section 2, we discuss the local fiber structures of *in vitro* 30 nm fibers and the relation to the fibers *in vivo*. In section 3, we discuss some of the polymer models that were introduced to describe the organization of the chromatin fiber on large scales. We argue that the simplest way to describe the fiber is by separating the condensation itself from the organization and show that the resulting model is good enough to explain the existing data. Finally, in section 4, we discuss possible mechanisms for the condensation of the fiber.

## 2. The 30 nm chromatin fiber

Most of what is known about the 30 nm fiber is through *in vitro* experiments. A large number of theoretical models for the 30 nm fiber have been put forward, all of them being more or less compatible with the experimental data. Only very recently, the assembly of very regular reconstituted fibers brought such high demands on the models that many of them could be invalidated. In this section, we will comment on the various models that have been proposed. Furthermore, we stress the important role of the energetics of linker DNA bending and of nucleosomal interaction in determining the fiber structure. We discuss how the tails play an important part here and how a cell via their modifications can regulate the degree of fiber condensation.

### 2.1. Old models

Since 30 nm fibers are rather dense, EM images are open to a plethora of interpretations (cf [6] for a recent review on some of the proposed models). Early EM images, obtained by Finch and Klug in 1976 [7], showed repetitive bands with a spacing of around 110 Å that were almost orthogonal to the fiber axis, whereas no substructures seemed to be present along these bands. This observation suggested a solenoidal arrangement of the nucleosome and with this *solenoidal* model, the first chromatin fiber model was born. In order to have successive nucleosomes along the helical path in contact, the linker DNA has to be strongly bent, especially for 'short' linker lengths. Structural stability thus requires strong NCP–NCP interactions with the result that the fiber diameter is expected to be independent of the linker length. Although there is no specific argument known why the solenoidal arrangement has a specific diameter, experiments indicating a diameter that is independent of the linker length are seen as supporting the solenoid model. Recent single molecule experiments by Kruithof *et al* [8] showing a linear force–extension relation of the chromatin fiber over a rather large range of extensions also point in the direction of a solenoid arrangement.

Recurring patterns where nucleosomes seem to stack along two rows, with linker DNA tracing out a *zig-zag* pattern, both in intact [9] and nuclease-digested isolated chromatin [9, 10], led Worcel *et al* [10] and Woodcock *et al* [9] to propose the so-called *twisted ribbon* models. Cryo-electron microscopy indicated that linker DNAs are essentially straight [4], at least at low salt concentrations. This information gave support to the so-called *crossed-linker* models [11] that assume non-sequential folding of the NCPs connected via straight linkers that crisscross the interior of the fiber. Such a fiber structure is set by the linkers and not by the NCPs so that the fiber diameter continuously depends on the linker length (for details, see the discussion of the two-angle model in [2]). Slight variations in the linker length produce irregular fibers similar to those observed for native chromatin [12]. By cross-linking the nucleosomes before digesting the linker DNA with nuclease, Dorigo *et al* [13] came to the conclusion that the fiber must be of the two-start type.

### 2.2. Ribbon model

The models we discussed so far either do not predict the diameter of the fiber (solenoid model) or predict a diameter that varies with the linker length (crossed-linker model). The state-of-the-art experiment [14] on the dependence of the fiber diameter on the linker length makes use of the fact that the affinity for nucleosomes depends on the specific sequence of basepairs that wrap around the octamer [15]. This fact allows one to construct DNA templates on which equally spaced nucleosomes are formed [16]. Based on this method, Robinson *et al* [14] produced regular reconstituted chromatin fibers with varying repeat lengths of 177–237 bp, increasing in steps of 10 bp. Their EM measurements revealed a constant diameter of 33 nm, and a nucleosome line density (NLD) varying between 0.9 and 1.2 nucleosome per nm, for repeat lengths from 177 up to 207 bp. For the longer repeat lengths the diameter was 44 nm, the NLD increasing to a range of 1.3–1.5 $\text{nm}^{-1}$. These results suggest that it is not the length of the linker DNA that sets the fiber diameter, in contrast to the prediction of the crossed-linker model. Instead, these findings support the view that it is the arrangement of the nucleosomes that somehow favors a discrete set of fiber diameters (namely 33 and 44 nm). The linker DNA length enters only as a second-order effect that determines which one of the two fiber diameters is chosen.

This leads to the important question of why there is a discrete set of preferred nucleosomal arrangements. To answer this question, Depken and Schiessel [17] studied all possible fibers with densely packed nucleosomes. By mapping the chromatin cylinder to a strip with the long sides being identified, it is straightforward to show that dense packings are achieved by placing the nucleosomes in ribbons. Different possible dense packings can then be characterized by the number of ribbons. This leads to a discrete set of ribbon models, all of them, however, still having an infinite, continuous range of possible diameters. What changes locally on the nucleosome level, when the diameter is changed, is the effective wedge angle between neighboring nucleosomes in a ribbon. It is known from experiments that NCPs under certain conditions form arcs made out of a stack of NCPs where each NCP acts as a wedge with a wedge angle of 8°

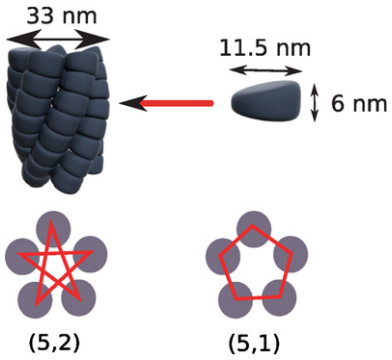


**Figure 1.** A 5-ribbon fiber with two connection schemes, (5, 2) and (5, 1).

**Table 1.** Relation among the number of ribbons, fiber diameter and NLD.

| Ribbons | Diameter (nm) | NLD (nucleosomes nm$^{-1}$) |
|---|---|---|
| 3 | 23 | 0.54 |
| 4 | 28 | 0.74 |
| 5 | 33 | 1.0 |
| 6 | 38 | 1.2 |
| 7 | 44 | 1.5 |

[18]. Assuming that this is also the ideal wedge angle inside a chromatin fiber, one can predict a discrete set of diameter/NLD combinations depending exclusively on the number of ribbons (table 1). Note that two of the predicted fibers, the 5-ribbon and the 7-ribbon structures, have diameters that coincide precisely with the experimental values of 33 and 44 nm. The 5-ribbon nucleosomal shell can be seen in figure 1.

In addition, one also has to specify the connectivity of the nucleosomes. If one assumes a regular connection which is identical for each pair of connected nucleosomes and where the fiber is not built out of disjoint filaments, the connectivity can be characterized by two numbers, $N$ and $m$. An $(N, m)$-fiber is then a fiber with $N$ ribbons where the linker DNA connects ribbons that are $m$ steps apart. One can then show that for fibers with 1, 2, 3, 4 and 6 ribbons, the only possible connectivity is that where neighboring ribbons are connected, $m = 1$. In this notation, the solenoid model is a (1, 1)-fiber and a twisted ribbon is a (2, 1)-fiber. The 5-ribbon structure has besides its nearest neighbor connectivity, (5, 1), also the next nearest neighbor connectivity, (5, 2), available. The 7-ribbon model allows for (7, 1), (7, 2) and (7, 3).

Why do the experiments of Robinson *et al* [14] indicate fiber diameters compatible with a dense 5-ribbon fiber for shorter linker lengths and with a 7-ribbon fiber at longer lengths? In [17] it is argued that the best of all possible structures is (5, 2) since this, at least for the shortest repeat length, allows for relatively straight linkers. However, when a repeat length of 217 bp is reached, the estimated volume of the linker DNA becomes larger than the volume available inside a 5-ribbon shell. At that value of the linker length the linker is just long enough to form a (7, 3) structure with straight linkers whereas the only available 6-ribbon fiber would require strong linker bending. Finally, let us mention that in a recent experiment a 167 bp repeat length was also probed, resulting in a 21.3 nm wide fiber with an NLD of 0.56 nucleosome nm$^{-1}$ [19]. This might point to a 3-ribbon structure. The small discrepancy can be attributed to the approximations involved in the model that start to matter at such small fiber diameters.

### 2.3. Energetics: elasticity and electrostatics

One important property we need to address is the energetics involved in the models. It is usually inferred from experiments that the linker histones are crucial [20, 19]. For example, Routh *et al* [19] deduced from EM measurements and sedimentation rates that reconstituted chromatin fibers with 197 bp repeat length *without* linker histones do not condense into a 33 nm fiber, but into a less dense structure. Pulling experiments in the pico-Newton range [8] suggest nonetheless that at low forces, such fibers have the same force–extension behavior with or without linker histones. Fibers without linker histones show, however, a transition to a more open structure at a lower force value than fibers with linker histones. This suggests a stabilizing role of the linker histones. The conflicting results of Routh *et al* might reflect the preparation for the EM measurements and the floppiness of the structure in the case of the sedimentation measurements.

In both cases, solenoid and crossed-linker model, the energy needed to bend the linker DNA can be estimated, assuming that DNA behaves like a wormlike chain for these contour lengths. The linker lengths range from 3.3 nm to 13 nm for 30 nm fibers with linker histones and are, except for the shortest value, clearly longer than the helical repeat of the double helix. For the solenoid model, the elastic energy can be as high as 35 kT per nucleosome. This high value actually suggests that the solenoidal structure, especially its diameter, would change with the linker length to reduce the elastic penalty. At first sight a 5-ribbon structure would encounter similar problems, but here the ribbons can slide with respect to each other without changing the fiber diameter or NLD, lowering the elastic energy to a few kT per nucleosome, the exact value depending on parameters such as the stem length and the exit angle by which the linker DNA leaves the stem.

It is not only the elastic energy that needs to be accounted for; there is also strong electrostatic repulsion between the negatively charged linkers. The above-mentioned pico-Newton pulling experiments by Kruithof *et al* indicate that the presence of magnesium ions is indispensable for the formation of a 30 nm fiber. This can be most likely attributed to the strong electrostatic repulsion that affects the linkers in a dense fiber. What the high density of nucleosomes suggests is that there is an effective attraction between NCPs that dictates the fiber condensation. This is the subject of the following section.

### 2.4. Energetics: nucleosome attraction

In the experiments by Dubochet and Noll in 1978 [18], it was found that isolated NCPs under controlled ionic conditions show a strong tendency to self-assemble into arcs and cylinders, and this in the absence of magnesium. The NCPs are stacked ‘face to face’, indicating the importance of nucleosome interactions in the formation of higher order

structures. As a possible mechanism behind the nucleosomal attraction the formation of tail bridges was later put forward, where positively charged tails of one nucleosome interact with negative charges on the core of a NCP closeby.

The tail conformations result from competition between electrostatics and entropy. For low salt concentrations, tails are condensed onto their nucleosome, whereas for higher salt concentrations, the entropic contribution of the tails to the free energy becomes more important. The tails gradually unfold with increasing ionic strength, and the effective diameter of the NCP saturates around physiological salt concentrations [21]. Osmometric measurements on dilute solutions of NCPs show a minimum in the second virial coefficient around the same salt concentration [22]. This led Mangenot *et al* [22] to suggest that the tails give the dominant contribution to the interaction between nucleosomes. More recently, Bertin *et al* [23] found that tail-intact NCPs show attraction in the absence of magnesium, with the second virial coefficient being in qualitative agreement with Mangenot *et al*, whereas it approached the hard-sphere repulsive interaction for NCPs where the tails were removed with trypsin. Moreover, for trypsinized oligonucleosomes it has been observed that no higher order folding occurred for an increase in monovalent salt [24] or magnesium concentration [25].

To understand better how the tails induce an effective attraction, Mühlbacher *et al* [26] modeled the NCPs as freely rotating spheres with a homogeneous surface charge distribution representing the histone–DNA core of the NCP. The eight tails were modeled as identical flexible chains grafted onto the sphere at the vertices of a cube inscribed in the sphere. The screened electrostatics was approximated by the Debye–Hückel interaction. For an appropriately chosen effective sphere charge, the pair potential showed an effective attraction of a few kT around physiological salt concentrations. Importantly, this attraction disappeared when a small fraction of the tail charges was removed, hinting at a possible biochemical mechanism through which the cell can control the nucleosomal interaction.

### 2.5. The 30 nm fiber in vivo

Until now we have discussed an idealized 30 nm fiber, mostly based on very regular reconstituted fibers under clean static conditions. It is an open question how relevant these structures are for the properties of chromatin within the nucleus. Bystricky *et al* [27] measured how the spatial distance (SD) depends on the chemical distance (CD) along the DNA double helix in budding yeast, using fluorescence *in situ* hybridization (FISH) for CDs from 14 kb (kilo basepairs) up to 100 kb. We will adhere here to the convention of expressing the CD in a number of basepairs, each basepair contributing a 'length' of 0.35 nm.

Before we discuss the FISH data, we need to address the reliability of 3D-FISH measurements. The main steps of FISH consist of a fixation step (using buffered formaldehyde), a denaturation step (by heating up the sample to 75 °C for 2 min) followed by a hybridization step where a fluorescent probe is matched to a specific sequence of the (denatured) DNA. Obviously, these procedures are rather harsh. Recent experiments [28, 29] set up to evaluate the reliability of FISH experiments came to the conclusion that large-scale structures, down to light microscopic resolution, are reasonably well preserved for this 3D-FISH. The older '2D-FISH', based on methanol/acetic acid fixation, seems to be significantly less reliable. On a smaller scale, both procedures are destructive and reliability suffers.

Keeping these restrictions in mind, Bystricky *et al* [27] could fit their data with the curve of a wormlike chain with a persistence length of 170–200 nm and an NLD of 0.64–0.91 nucleosomes $nm^{-1}$. Apparently, a rather stiff condensed fiber is formed but how it relates to the original *in vivo* structure is an open question. Nonetheless, the persistence length inferred from the experiment is in relatively good agreement with coarse grained models of the 30 nm fiber [5, 30]. Especially from the simulation in [5], one can draw the not-so-surprising conclusion that the worm-like chain model is only appropriate for small bends. Kinks can be formed with relatively low cost. This last point has to be kept in mind when discussing large-scale structures to which we will turn in the next section.

### 2.6. Conclusion: the 30 nm fiber

The existing models of the 30 nm fiber should be regarded as a description of a ground state of the chromatin fiber in the nucleus. The reconstituted fibers form an interesting playground to get a grip on the possible energies that play a role in the formation. It is important to realize that in the nucleus, the chromatin fiber gets synthesized in a way different from that of reconstituted fibers. The *in vivo* fiber is also not as regular and static as the reconstituted fibers. Although the fiber is often thought of as a wormlike chain, it should be kept in mind that the notion of a persistence length is only valid as some kind of rough average. The flexibility has most likely large variations and the fiber is highly extensible. We will not rely on any specific persistence length for the following section. When there is a need to compare values with the Kuhn length of the chromatin fiber we will use a value of 300 nm, realizing that one could argue as well for lengths ranging from 60 [31] to 400 [27] nm.

## 3. Large-scale structures

By analyzing the local radiation damage of chromosomes [32], Cremer *et al* concluded—in contrast to the general picture at that time—that during interphase chromosomes are segregated within their own domain. Most of the evidence of the existence of these separate chromosome domains comes from FISH data. As we have discussed before, the resolution of these data is restricted to the optical, not only because of the measurement apparatus but also due to the preparation procedure. Although there is some evidence that intermingling of chromatin domains does occur [33], recent experiments point in the direction of domains that at least do not intertwine [34]. The section discusses the structure of chromosomes in their own domain.

### *3.1. Experiments and models*

The use of FISH to examine the distribution of chromatin in interphase nuclei dates back to van den Engh *et al* [35]. They measured via 2D-FISH the SD versus the CD for many pairs of probes. In a first analysis of their data, they noted that they could fit them to a Gaussian chain up to 2 Mbp of CD. For longer CDs, a flattening of the curve was found indicating the existence of some constraint. This analysis was worked out in greater detail by Hahnfeldt *et al* [36] where the data were fitted to a Gaussian chain within a spherical confinement. Extension of these 2D-FISH measurements on the same chromosomes up to 190 Mbp [37] again showed for larger CDs the footprint of a random walk but with a considerable smaller slope of CD versus the squared SD. The data were fitted to a fixed Mbp giant loop model with the loop nodes forming a long distance random walk. It was argued that this is the simplest model to explain the new data.

These same data led Münkel and Langowski [38] to propose their multi-loop subcompartment model as a Gaussian chain with a non-hardcore volume interaction together with harmonic bonding into loops. A compartment of loops is then attached to the next compartment by a chromatin link. Their idea was first of all to emulate the formation of clearly separated subcompartments within a chromosome territory. Several characterizations of these subcompartments exist. We will use the terminology 'euchromatin' for the less dense, gene active regions and 'heterochromatin' for the denser, inactive regions. Other not fully compatible terms are R-band/G-band (based on Giemsa staining) [39], ridge (regions of increased gene expression)/antiridge [40], depending on one's taste, measurement technology or functionality. A special feature of this model is that, according to the authors, it replicates the scaling of the SD as a function of the CD over large distances, and *not* as a polymer at its $\theta$-point (a random walk with exponent $1/2$) *nor* as a polymer in a good solvent (a self-avoiding random walk with exponent $3/5$), but with an exponent of $1/3$, from which they inferred that it behaves like a globule.

More recent 3D-FISH measurements [41] differentiated between distances within euchromatin and heterochromatin regions of chromosomes in human fibroblast cells. The authors noted that they could fit their data to a globular state with exponent $1/3$ but also observed a leveling off to a constant value for larger CDs. The size of this leveling off was significantly different for different regions, strengthening the idea that non-active regions are considerably denser than active ones. The above-mentioned leveling off led Bohn *et al* [42] to propose yet another loop-based model, the random loop model: a chain with beads connected by a harmonic potential, a Gaussian chain, without volume interactions, but where a harmonic attraction of the same strength as the chain links is introduced between non-neighboring beads with a fixed probability. The authors claimed that such a random loop configuration is needed to explain the leveling off, and it again reproduces the $1/3$ exponent.

### *3.2. The loop and the globule*

In this subsection, we attempt to critically analyze the models that we briefly discussed in the previous subsection. Our starting point is the fact that the chromatin fibers within the nucleus and also within their compartments are highly confined. We now separate this notion of confinement from the spatial distribution of the chromatin, somewhat in the spirit of the spherical confinement model. The possible mechanism behind this confinement will be discussed in the following section. The logic behind this approach is that it is not known what causes the confinement, let alone the details behind it. As will become clear, we also do not need this knowledge to explain the data presented so far. This also means that we will not assume any loop formation, leaving the causality between confinement and loop formation open.

To set the stage, let us estimate the density of the chromatin fiber in a human cell. Human lymphocytes have a nuclear volume between 380 and 525 $\mu$m$^3$ [43]. Let us assume that the chromatin is spread throughout the nucleus, neglecting the space taken up by nuclear organelles like the nucleoli or other non-chromatin domains. We expect this approximation to be sufficient in view of the precision of the experiments we aim to describe here. With an NLD of 0.7 nm$^{-1}$, a repeat length of 200 bp and a fiber diameter of 33 nm, a 380 $\mu$m$^3$ nucleus corresponds to a chromatin volume fraction of almost 0.1. The first fact that needs to be understood is why a pure random walk can explain the data this well (up to lengths before confinement/loop forming sets in). After all, the chromatin fiber has a large cross section. It could be a coincidence that attractive forces just balance the repulsive forces and the Kuhn length could be much shorter than what we would conclude from a persistence length of around 150 nm. In that case, it makes one wonder how this could be achieved with varying densities. It is appropriate to introduce some (old) polymer physics at this point.

Let us suppose that chromatin is highly confined but in a reasonably good solvent. When we start to follow the chromatin fiber from a given point, for length scales up to its persistence length, the relation between the SD and CD will be approximately linear. For longer contour lengths, there will be a crossover to a random walk followed by a crossover to a self-avoiding random walk (SAW) when the effective strength of the volume interactions becomes equal to the thermal energy. This defines the 'thermal blob' size. Finally at length scales larger than the correlation length, density fluctuations disappear and there is no preferred direction. This correlation length is just set by the distance where collisions with segments nearby CD and segments far away, i.e. for large CDs, are as likely. It should be noted that the segment density can be so high that the correlation length is smaller than the thermal blob size in which case the crossover to the SAW does not occur.

We will derive the correlation length following [44]. The expectation value for the segment density, $C_0$, is constant within a compartment. This is in fact only true neglecting boundary effects, but with the relatively high densities in the nucleus this is a reasonable assumption. Starting from one segment at the origin, in its proximity the segment distribution

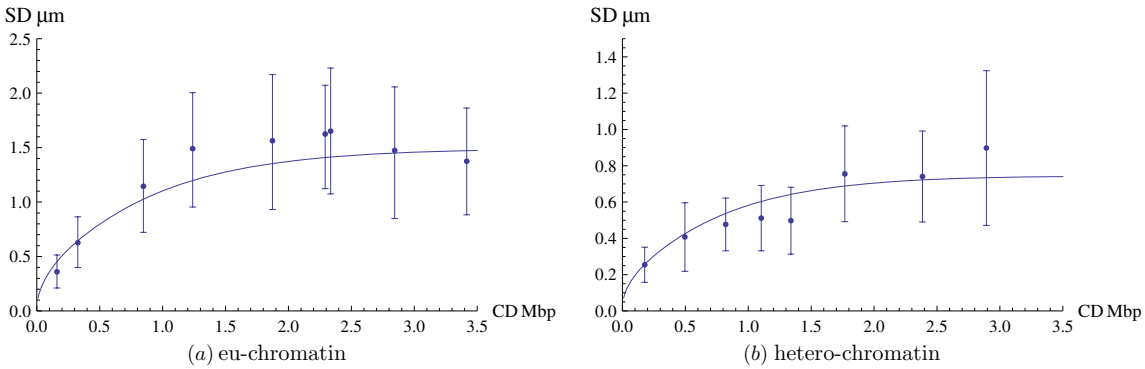


(*a*) eu-chromatin (*b*) hetero-chromatin

**Figure 2.** 3D-FISH data from [41] for the (*a*) active and (*b*) non-active regions of chromosome 1 in fibroblasts. The error bars are the standard deviations. The curves use (7) with the parameters being given in the main text.

can be divided into a contribution coming from segments close by along the backbone, $c_c$, and segments far away, $c_f$, both strongly fluctuating on small scales:

$$C_0 = \langle c_c(r) + c_f(r)\rangle = \langle c_c(r)\rangle + \langle c_f(r)\rangle. \tag{1}$$

Now suppose that the solution is dilute enough such that excluded volume effects become important before the semi-diluteness of the solution becomes relevant. Close to the origin, the density is dominated by the first term and the presence of faraway segments can be neglected. $N$ segments of the chain with volume interactions then have a radius of gyration that scales as

$$R \approx a\left(\frac{v}{a^3}\right)^{1/5} N^{3/5}, \tag{2}$$

where $a$ is the Kuhn length and $v$ is the excluded volume. From this expression follows as segment density:

$$\langle c_c(r)\rangle \approx \left(\frac{a^3}{v}\right)^{1/3} a^{-3}\left(\frac{r}{a}\right)^{-4/3}. \tag{3}$$

The faraway contribution kicks in when the first term becomes of the order of the overall density. This defines the correlation length $\xi$:

$$\frac{\xi}{a} \approx \left(\frac{a^3}{v}\right)^{1/4} (C_0 a^3)^{-3/4}. \tag{4}$$

On length scales larger than $\xi$, the density fluctuations are minimal and the chromatin is in the globular state. Although it is true that the size of a globule scales as (number of monomers)$^{1/3}$, it is a misconception that locally the distance between segments scales with (number of connecting segments)$^{1/3}$. It is an old argument by Flory [45] that points to an exponent of $1/2$ in this case, namely the pressure from all directions is the same, because of the homogeneity of the globule, and so there are no effective volume effects. The chain thus forms a random walk of 'blobs' with the blob size being given by the correlation length. Although there are some deviations at short length scales to this 'Flory ideal chain hypothesis', it was recently shown by Lua *et al* [46]—using an ingenious counting algorithm on a lattice—to hold more than well enough. The only drawback of that simulation when applied to our problem is that it presupposes that the system is ergodic and that the system has time to thermalize. This last point might be important, as we will discuss at the end of this section.

Let us consider in this context the more recent 3D-FISH data for chromosome 1 in human fibroblast [41]. The only data available are the average SD as a function of the CD *and* the standard deviation, both depicted in figure 2. Knowing other moments might reveal more detail. As mentioned before, the SD levels off at larger CDs. We expect that the height of the plateau corresponds to the average distance between two points in the compartment:

$$\langle \mathrm{SD}\rangle = \frac{1}{V^2}\int_V \mathrm{d}^3\vec{r}_1 \int_V \mathrm{d}^3\vec{r}_2 |\vec{r}_1 - \vec{r}_2|. \tag{5}$$

For example, for a spherical compartment of radius $R$, we find an average of $(36/35)R$ and a standard deviation of $\sigma = (\sqrt{174}/35)R \approx 0.38R$, while for a flat disk with radius $R$ the average distance is $0.9R$ with a standard deviation of $0.42R$. Human fibroblast has an almost 2D nucleus which can also be inferred from the FISH measurements over the whole chromosome 1 [41]. For a length of 30 Mb, there is a leveling off around 1.8 $\mu$m. Using a volume fraction of 0.1, a repeat length of $r_l = 200$ bp and an NLD of 0.7 nm$^{-1}$, one predicts a value of 150 nm of the thickness for a disk-shaped compartment.

It is important to realize that although the globular state has local Gaussian behavior, it is not to be confused with a Gaussian chain confined to the region of a globule, the structure assumed in [36]. The latter has a strong density peak in the center of the confinement [45], while here we have a constant density profile. The reason for this difference is that the confined Gaussian is Gaussian because of the *lack* of volume interactions while in the case of a globule, it is Gaussian *because* of volume interactions. This distinction is not always appreciated. Were we to repeat the calculation for the average distance and standard deviation using the confined Gaussian probability, $\rho(r) = \sin\left(\frac{\pi r}{R}\right)\big/(\pi R r^2)$, we would find for the height of the plateau and its standard deviation:

$$\langle \mathrm{SD}(\mathrm{CD}\to\infty)\rangle_{\mathrm{Gauss}} \approx 0.7R \qquad \sigma_{\mathrm{Gauss}} \approx 0.14R. \tag{6}$$

We would clearly get a higher estimate of the size of the compartment. It is interesting to note that the *relative* standard deviation is 0.2, considerably smaller than 0.38 for the globule. When we compare this with the plateau of chromosome 1,

for both eu- and heterochromatin compartments, we see a relative standard deviation of 0.37 indicating that the picture of a globule describes this in a satisfactory way.

In the following, we model the chromatin within its compartment as a Gaussian chain within a rectangular box. To ensure a flat density profile, we have to choose reflecting boundary conditions. The mean-squared SD is then given by

$$\langle(\mathrm{SD}(\mathrm{CD}))^2\rangle = \frac{1}{V}\left(\frac{3}{2\pi L(\mathrm{CD})b}\right)^{3/2} \times \int_V \mathrm{d}^3\vec{r}_1 \int_V \mathrm{d}^3\vec{r}_2 (\vec{r}_1 - \vec{r}_2)^2 \tag{7}$$

$$\sum_{n_x,n_y,n_z=-\infty}^{\infty} \left[\exp\left(-\frac{3(\vec{r}_1 - f_{\vec{n}}(\vec{r}_2))^2}{2L(\mathrm{CD})b}\right)\right], \tag{8}$$

where

$$f_{\vec{n}}(\vec{r})_i := (-1)^{n_i}(r_i - n_i L_i) \tag{9}$$

takes care of the reflections. The number of reflections is counted by $\vec{n}$ in each direction. The quantity $b$ is the step length of the random walk and $L(\mathrm{CD})$ is its length. A natural choice for $b$ is the correlation length. In that case, $L(\mathrm{CD})$ would be the contour length of the random walk of correlation blobs. The problem here is that we do not know the functional relationship $L = L(\mathrm{CD})$. Let us use the contour length of the chromatin fiber, using the same values as above. The size of the box we choose is $4 \times 4 \times 0.15\ \mu\mathrm{m}^3$. Fitting the curve of $\sqrt{\langle(\mathrm{SD}(\mathrm{CD}))^2\rangle}$ to the 3D-FISH data [41] we extract a step size of $b = 300$ nm, agreeing with the Kuhn length for the chromatin fiber. This seems to be too good to be true! We can also estimate the correlation length using (4). We again assume $a = 300$ nm as the Kuhn length and a rigid rod excluded volume of $v = a^2 d$ *à la* Onsager [45], where we take $d = 30$ nm as the diameter. This results in an effective segment volume of $\pi d^2 a/4\ \mathrm{nm}^3$. If we again assume a volume fraction of 0.1, we get a correlation length of 80 nm. This seems to be considerably smaller than what the fit indicates, especially after realizing that the correlation length is *shorter* than the Kuhn length on which we based the calculation. In fact we find for the thermal blob size the size up to which a non-confined chain can be considered ideal, using the same fiber parameters as above, a value larger than 1 $\mu$m. In this picture, SAW scaling will be absent over the whole range. This changes the formula for the correlation length: using ideal chain scaling up to the correlation length results in a correlation length of

$$\frac{\xi_{\mathrm{ideal}}}{a} \approx \frac{1}{C_0 a^3}. \tag{10}$$

With the same values as above we now find a correlation length of 24 nm, even smaller than before. It seems to be likely that the actual Kuhn length is considerably smaller than 300 nm. This point nicely illustrates that the data available at the moment do not justify detailed models.

We can repeat the same calculations for a heterochromatin region. The resulting fit for a random walk step length of $b = 120$ nm is depicted in figure 2(*b*). The compaction of the heterochromatin is 2, 5 (equation (10)) times higher in this naive view.

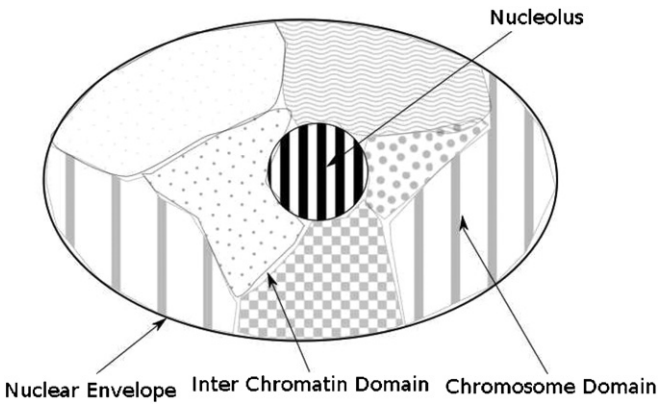


**Figure 3.** Schematic view of the nucleus of an eukaryotic cell.

Although the concept of a globule seems to fit the data well, this is somewhat deceptive. First of all, FISH data are not very reliable. Higher moments might reveal more structure than a globular state. One should also not forget that the nucleus is never in equilibrium. Active processes do influence the distribution of chromatin and the cell continuously evolves through its cell cycle. An interesting example is a recent simulation by Rosa and Everaers [47] where the interphase structure is a consequence of the fast decondensation of structured mitotic chromosomes within the confinement of the nuclear envelope, whereas the timescale of equilibration is much longer than the duration of interphase. The consequence is that the chromatin fiber is not thermalized. Although they compare their simulations with rather unreliable 2D-FISH data, the authors demonstrate how the nonequilibrium conditions in the nucleus can influence the spatial distribution of chromatin.

### *3.3. Conclusion: large-scale structure*

The techniques available, or at least used so far, to reveal the large-scale organization of chromatin do not, in our opinion, justify any detailed polymer model. One can capture most of the features with the statement that chromatin exists in a condensed state. New techniques will hopefully make it possible to refine this picture.

## 4. Mechanism behind compactification

As we have seen, the chromosomes within the nucleus are more or less confined, each in its own domain (see figure 3). These domains are much smaller than the typical size of a chromatin fiber in a good solvent. The amount of compactification in interphase is furthermore not constant but varies considerably between regions containing active genes and less active regions.

Within the cell cycle, a dramatic increase of compactification is apparent when the cell enters metaphase. This change from dispersed interphase chromosomes toward compactified mitotic chromosomes during prophase is fast and remarkably synchronous.

The question one has to ask is: what are the forces involved in compactifying the chromatin inside the nucleus, depending on its activity during interphase and into mitotic chromosome during mitosis, while keeping different chromosomes separated? At the same time, these forces might be also somehow relevant for sister chromatid segregation after replication.

One factor we will not consider here are active processes that could take part in condensing or decondensing chromatin. We like to think that these factors work on top of a more general mechanism.

### *4.1. Enclosure*

At first thought one might think that the chromatin is confined by the nuclear envelope, the double membrane encapsulating the nucleus. This was assumed in a recent simulation where it was also pointed out that the timescale of the cell cycle is too short for the expanded chromatins to thermalize [47] and especially to mix. This is an attractive scenario, especially reminding us that the organization of chromatin is probably never in equilibrium.

Purely by enclosing the nucleus it is, however, not possible to regulate the densities depending on gene activity. Especially, some regions in the nucleus seem to be chromatin-free without any membrane separating them from the chromatin-containing regions [34, 48]. Finally, there is still the need for a mechanism to condense the chromatin for mitosis.

### *4.2. Specific binding sites*

Two somewhat overlapping models start from a more or less rigid backbone of proteins or protein filaments.

*4.2.1. Nuclear matrix.* The nuclear matrix (for a review, see [49]) is conceived to be a network of filaments that span the nucleus reminiscent of the cytoskeleton in the cytoplasm. The idea is that this network is responsible for the organization in chromatin compartments. The chromatin is supposed to be attached to this network through specific sequences along the genome appropriately named MARs or matrix attachment regions, some not precisely known, presumably AT rich regions. An important problem with this model is that the network itself has never been indisputably detected and it is often defined as 'the stuff that is left behind within the nuclear envelope when all other material has been extracted'. The electron microscope images suggesting such a structure could suffer from artifacts caused by sample preparation. A second objection is the variable position of each chromosome from cell to cell [32] that makes the existence of such a well-defined nuclear matrix less likely.

Finally, a large number of specific MARs slightly contradicts the notion of robustness under mutation and of the constrained diffusion of chromatin observed during interphase [50]. It is nonetheless very well possible that some parts of the chromosome are localized with respect to the nuclear envelope. Conceptually this seems likely at least for the centromere, it being the only part of the chromatin that needs to be localized during mitosis.

*4.2.2. Scaffold.* The idea that a rigid protein scaffold organizes the chromosomes originates from EM pictures of mitotic chromosomes depleted from histones using high salt concentrations [51]. A core of non-histone proteins in the shape of the original mitotic chromosome remains with a halo of bare DNA loops attached to it. The main constituents of this scaffold were later found to be topoisomerase II [52] and condensin [53], the former being a protein complex responsible for disentangling DNA and the latter being a complex closely related to the cohesin complex that keeps the two sister chromatids bound together up to telophase [54]. The picture that evolved was that of loops of chromatin attached to the protein scaffold through specific AT rich regions called SARs (scaffold attachment regions). The notion of a scaffold has some overlap with the previously mentioned nuclear matrix and not too surprisingly the weak points of the matrix concept carry over to the scaffold.

A strong argument against the structural importance of a mitotic scaffold can be drawn from experiments by Poirier and Marko in 2002 [55], where it was found that the mitotic chromosome loses its structural integrity by gradually cutting the DNA with nuclease, showing that the chromatin fiber defines the structure of the chromosome, making the existence of a scaffold unlikely. Moreover, it was already known that topoisomerase II was not needed for the formation of the mitotic structure [56]. In 2006 it was found, surprisingly, that the same holds for condensin. The main function of condensin seems to be the stabilization of the mitotic chromosome during telophase [57].

### *4.3. Non-specific compactification*

*4.3.1. Electrostatics.* An alternative to these local types of mechanisms is the idea that attractive interactions between segments of the chromatin fiber dominate the hardcore-like repulsive forces in such a way that the second virial coefficient becomes negative, turning the effective background of the chromatin into a poor solvent. This attraction could be caused by a tail bridging effect, as we have discussed above between nucleosomes and/or mediated by dynamically chromatin binding proteins.

There are some suggestions in the literature [58] that the environment in the nucleus is such that most counterions of even strong polyelectrolytes are condensed, caused by the lack of free water. Measurements on several different cell types do not support this view.

- The water content of the nuclei of amphibian oocytes was measured to be around 74–80% of mass [59] and over 85% of rat liver cells [60].
- NMR measurements [61] of frog (Xenopus Laevis) oocytes showed that almost 90% of the water present in the nucleus can be considered free.
- Even the water content of the highly condensed mitotic chromosome was estimated to be at least one-third of the volume [62].

At this stage, there is no reason to believe that the electrochemical conditions within the nucleus differ much from what one considers physiological.

- The nuclear envelope contains a large number of nuclear pores, typically around 3000, but in certain oocytes up to 50 million [63]. These pores are fully permeable for particles up to 9 nm in diameter [64].
- The 30 nm chromatin fiber as seen *in vitro* under 'physiological' conditions closely resembles the fiber-like structure seen in FISH experiments [27], as explained before.
- As mentioned above, NCPs seem to be tuned for minimizing their second virial coefficients at 'physiological' salt concentrations.
- Extracted mitotic chromosomes appear to have their *in vivo* dimensions at 'physiological' conditions, reversibly condensing or decondensing with a change in salt concentration [62].
- Upon hypertonic shock the chromatin partly condenses [34], indicating a strong dependence on salt concentration.

The change in the level of compactification is correlated with some of the histone modifications. A typical example is H3 phosphorylation during mitosis [65]. The same phosphorylation is correlated with the formation of heterochromatin [66]. It is possible that some of the modifications have a direct effect on the interaction between segments of the chromatin fiber through changes in the charge of the tails. Alternatively, they could affect the binding of proteins that mediate the electrostatic interaction.

A somewhat puzzling feature is the formation of the aforementioned hypercondensation caused by an increase of salt concentration, a condition that weakens the range of the electrostatic forces through increased screening. Another point that is still hard to understand is how this subtle balance between attractive and repulsive forces can be maintained over such a large variety of cells and organisms.

*4.3.2. Crowding.* The notion of crowding in biology [67] corresponds roughly to the notion of depletion in colloid physics. For the case that the colloids are much larger than the polymers, the so-called colloid limit, the effective attraction between the colloids, is reasonably well understood [68]: when two colloids are separated by a distance shorter than the size of the polymer, the osmotic pressure of the polymers pushes the two colloids together. Subtleties arise from the ease with which two polymers can overlap [45] and from the appearance of a repulsive barrier when incorporating higher order interaction terms, but the main picture remains.

In the protein limit where the colloid is much smaller than the polymer, the situation is not that clear. This is the limit of interest for the condensation of chromatin in the nucleus. If we think of the chromatin fiber as being dilute in a good solvent or in a semi-dilute solution, the relevant length scale characterizing the fiber, namely the radius of gyration or the correlation length, is considerably larger than the typical size of the proteins (around 2.5 nm). In that case it was shown by DeGennes [69] that purely by excluded volume effects, polymers and nanoparticles with the size of an average protein are highly miscible. The conceptual reason is that the range of the depletion is then set by the size of the protein [70]. Since the cost of placing the nanoparticle within the polymer is expected to be proportional to the segment concentration, a scaling argument shows that this requires little work. In that case, the minimum of the depletion potential between two nanoparticles is also not deep enough to cause phase separation. This was also confirmed in experiments, where non-DNA binding proteins from E. coli extracts alone could not condense DNA [71], not even with concentrations considerably higher than what is found in eukaryotic nuclei. Another experiment that indicates that nanoparticles of the size of the average protein easily diffuse within the densest chromatin regions, even within the mitotic chromatin fibers, was conducted by Verschure *et al* [72].

Unless other effects decrease the excluded volume parameter of the chromatin fiber and/or increase the interaction between DNA and nanoparticles, depletion interactions seem to be too small to cause condensation of the chromatin fiber. A recent paper [73] discusses the possibility that charged nanoparticles, with the same charge as the polymer, could cause condensation in the spirit of Odijk's osmotic compaction [74] of the supercoiled DNA in E. coli. The negatively charged protein fraction needed seems to be too high to be realizable, without further ingredients, in the nucleus, where the overall non-histone protein fractions are 0.1–0.15.

## 5. Summary and outlook

It is clear that the eukaryotic nucleus is an extremely complex system. The biophysical approaches have made progress in the description of chromatin by building the models from a detailed description. At some point the barriers to be overcome seem, however, to be too hard to continue in this way. On the other hand, it seems logical that the robustness of the eukaryotic nucleus against changing conditions and mutations must have a general physical explanation. In this paper, we have discussed the strengths and the weaknesses of the common approaches toward an understanding of the cell cycle. We have shown that no detailed model is needed to explain the large-scale organization of chromatin observed so far. This notion makes it possible to separate the physics behind the organization from the detailed structure. We hope that this approach will lead to a better understanding of the cell cycle in the near future.

## Acknowledgments

We thank Theo Odijk, Jonathan Widom and John van Noort for the many insights and helpful discussions and John van Noort and Roel van Driel for making their measurements available. This research was supported by the Dutch Science Foundation NWO/FOM.

## Glossary

Chromatin, polymer models, large-scale organization, 30 nm fiber, compactification

## References


[1] Davey C A, Sargent D F, Luger K, Maeder A W and Richmond T J 2002 Solvent mediated interactions in the structure of the nucleosome core particle at a 1.9 resolution *J. Mol. Biol.* **319** 1097–113

[2] Schiessel H 2003 The physics of chromatin *J. Phys.: Condens. Matter* **15** R699–774

[3] Kulić I M and Schiessel H 2008 Opening and closing DNA: theories on the nucleosome *DNA Interactions with Polymers and Surfactants* ed R Dias and B Lindman (New York: Wiley) chapter 7, pp 173–208

[4] Bednar J, Horowitz R A, Grigoryev S A, Carruthers L M, Hansen J C, Koster A J and Woodcock C L 1998 Nucleosomes, linker DNA, and linker histone form a unique structural motif that directs the higher-order folding and compaction of chromatin *Proc. Natl Acad. Sci.* **95** 14173–8

[5] Mergell B, Everaers R and Schiessel H 2004 Nucleosome interactions in chromatin: fiber stiffening and hairpin formation *Phys. Rev.* E **70** 011915

[6] van Holde K and Zlatanova J 2007 Chromatin fiber structure: where is the problem now? *Semin. Cell. Dev. Biol.* **18** 651–8

[7] Finch J T and Klug A 1976 Solenoidal model for superstructure in chromatin *Proc. Natl Acad. Sci.* **73** 1897–901

[8] Kruithof M, Chien F-T, Routh A, Logie C, Rhodes D and van Noort J 2008 A highly compliant helical folding for the 30 nm chromatin fibre *Nat. Struct. Mol. Biol.* accepted

[9] Woodcock C L, Frado L L and Rattner J B 1984 The higher-order structure of chromatin: evidence for a helical ribbon arrangement *J. Cell. Biol.* **99** 42–52

[10] Worcel A, Strogatz S and Riley D 1981 Structure of chromatin and the linking number of DNA *Proc. Natl Acad. Sci.* **78** 1461–5

[11] Staynov D Z 1983 Possible nucleosome arrangements in the higher-order structure of chromatin *Int. J. Biol. Macromol.* **5** 3–9

[12] Woodcock C L, Grigoryev S A, Horowitz R A and Whitaker N 1993 A chromatin folding model that incorporates linker variability generates fibers resembling the native structures *Proc. Natl Acad. Sci.* **90** 9021–5

[13] Dorigo B, Schalch T, Kulangara A, Duda S, Schroeder R R and Richmond T J 2004 Nucleosome arrays reveal the two-start organization of the chromatin fiber *Science* **306** 1571–3

[14] Robinson P J J, Fairall L, Huynh V A T and Rhodes D 2006 Em measurements define the dimensions of the '30-nm' chromatin fiber: evidence for a compact, interdigitated structure *Proc. Natl Acad. Sci.* **103** 6506–11

[15] Lowary P T and Widom J 1998 New DNA sequence rules for high affinity binding to histone octamer and sequence-directed nucleosome positioning *J. Mol. Biol.* **276** 19–42

[16] Huynh V A T, Robinson P J J and Rhodes D 2005 A method for the *in vitro* reconstitution of a defined '30 nm' chromatin fibre containing stoichiometric amounts of the linker histone *J. Mol. Biol.* **345** 957–68

[17] Depken M and Schiessel H 2007 Nucleosome shape dictates chromatin-fiber structure *Biophys. J.* at press

[18] Dubochet J and Noll M 1978 Nucleosome arcs and helices *Science* **202** 280–6 (Nucleosome wedge-angle)

[19] Routh A, Sandin S and Rhodes D 2008 Nucleosome repeat length and linker histone stoichiometry determine chromatin fiber structure *Proc. Natl Acad. Sci.* **105** 8872–7

[20] Thoma F, Koller T and Klug A 1979 Involvement of histone h1 in the organization of the nucleosome and of the salt-dependent superstructures of chromatin *J. Cell. Biol.* **83** 403–27

[21] Mangenot S, Leforestier A, Vachette P, Durand D and Livolant F 2002 Salt-induced conformation and interaction changes of nucleosome core particles *Biophys. J.* **82** 345–56

[22] Mangenot S, Raspaud E, Tribet C, Belloni L and Livolant F 2002 Interactions between isolated nucleosome core particles: a tail-bridging effect? *Eur. Phys. J.* **7** 221–31

[23] Bertin A, Leforestier A, Durand D and Livolant F 2004 Role of histone tails in the conformation and interactions of nucleosome core particles *Biochemistry* **43** 4773–80

[24] Garcia-Ramirez M, Dong F and Ausio J 1992 Role of the histone 'tails' in the folding of oligonucleosomes depleted of histone h1 *J. Biol. Chem.* **267** 19587–95

[25] Fletcher T M and Hansen J C 1995 Core histone tail domains mediate oligonucleosome folding and nucleosomal DNA organization through distinct molecular mechanisms *J. Biol. Chem.* **270** 25359–62

[26] Mühlbacher F, Holm C and Schiessel H 2006 Controlled DNA compaction within chromatin: the tail-bridging effect *Europhys. Lett.* **73** 135–41

[27] Bystricky K, Heun P, Gehlen L, Langowski J and Gasser S 2004 Long-range compaction and flexibility of interphase chromatin in budding yeast analyzed by high-resolution imaging techniques *Proc. Natl Acad. Sci.***101**

[28] Solovei I, Cavallo A, Schermelleh L, Jaunin F, Scasselati C, Cmarko D, Cremer C, Fakan S and Cremer T 2002 Spatial preservation of nuclear chromatin architecture during three-dimensional fluorescence *in situ* hybridization (3D-FISH) *Exp. Cell. Res.* **276** 10–23 (FISH validity)

[29] Hepperger C, Otten S, von Hase J and Dietzel S 2007 Preservation of large-scale chromatin structure in FISH experiments *Chromosoma* **116** 117–33

[30] Wedemann G and Langowski J 2002 Computer simulation of the 30-nanometer chromatin fiber *Biophys. J.* **82** 2847–59

[31] Cui Y and Bustamante C 2000 Pulling a single chromatin fiber reveals the forces that maintain its higher-order structure *Proc. Natl Acad. Sci.* **97** 127–32

[32] Cremer T, Cremer C, Schneider T, Baumann H, Hens L and Kirsch-Volders M 1982 Analysis of chromosome positions in the interphase nucleus of chinese hamster cells by laser–uv–microirradiation experiments *Human Genet.* **62** 201–9

[33] Branco M R and Pombo A 2006 Intermingling of chromosome territories in interphase suggests role in translocations and transcription-dependent associations *PLoS Biol.* **4** e138

[34] Albiez H *et al* 2006 Chromatin domains and the interchromatin compartment form structurally defined and functionally interacting nuclear networks *Chromosome Res.* **14** 707–33

[35] van den Engh G, Sachs R K and Trask B J 1992 Estimating genomic distance from DNA sequence location in cell nuclei by a random walk model *Science* **257** 1410–2

[36] Hahnfeldt P, Hearst J E, Brenner D J, Sachs R K and Hlatky L R 1993 Polymer models for interphase chromosomes *Proc. Natl Acad. Sci.* **90** 7854–8

[37] Sachs R K, van den Engh G, Trask B J, Yokota H and Hearst J E 1995 A random-walk/giant-loop model for interphase chromosomes *Proc. Natl Acad. Sci.* **92** 2710–4

[38] Munkel C and Langowski J 1998 Chromosome structure predicted by a polymer model *Phys. Rev.* E **57** 5888–96

[39] Comings D E 1978 Mechanisms of chromosome banding and implications for chromosome structure *Ann. Rev. Genet.* **12** 25–46

[40] Caron H *et al* 2001 The human transcriptome map: clustering of highly expressed genes in chromosomal domains *Science* **291** 1289–92

[41] Mateos-Langerak J, Giromus O, de Leeuw W, Bohn M, Verschure P J, Kreth G, Heermann D W, van Driel R and Goetze S 2007 Chromatin folding in relation to human genome function (arXiv:0705.1656v1)

[42] Bohn M, Heermann D W and van Driel R 2007 Random loop model for long polymers *Phys. Rev.* E **76** 051805
[43] Cremer M, von Hase J, Volm T, Brero A, Kreth G, Walter J, Fischer C, Solovei I, Cremer C and Cremer T 2001 Non-random radial higher-order chromatin arrangements in nuclei of diploid human cells *Chromosome Res.* **9** 541–67
[44] Daoud M, Cotton J P, Farnoux B, Jannink G, Sarma G, Benoit H, Duplessix C, Picot C and de Gennes P G 1975 Solutions of flexible polymers. neutron experiments and interpretation *Macromolecules* **8** 804–18
[45] Grosberg A Yu and Khokhlov A R 1994 *Statistical Physics of Macromolecules* (New York: AIP)
[46] Lua R, Borovinskiy A L and Grosberg A Yu 2004 Fractal and statistical properties of large compact polymers: a computational study *Polymer* **45** 717–31
[47] Rosa A and Everaers R 2008 Structure and dynamics of interphase chromosomes *PLoS Comput. Biol.* **4** e1000153
[48] Cremer T, Küpper K, Dietzel S and Fakan S 2004 Higher order chromatin architecture in the cell nucleus: on the way from structure to function *Biol. Cell.* **96** 555–67
[49] Nickerson J 2001 Experimental observations of a nuclear matrix *J. Cell. Sci.* **114** 463–74
[50] Marshall W F, Straight A, Marko J F, Swedlow J, Dernburg A, Belmont A S, Murray A W, Agard D A and Sedat J W 1997 Interphase chromosomes undergo constrained diffusional motion in living cells *Curr. Biol.* **7** 930–9
[51] Paulson J R and Laemmli U K 1977 The structure of histone-depleted metaphase chromosomes *Cell* **12** 817–28
[52] Earnshaw W C, Halligan B, Cooke C A, Heck M M and Liu L F 1985 Topoisomerase ii is a structural component of mitotic chromosome scaffolds *J. Cell. Biol.* **100** 1706–15
[53] Hirano T, Kobayashi R and Hirano M 1997 Condensins, chromosome condensation protein complexes containing xcap-c, xcap-e and a xenopus homolog of the drosophila barren protein *Cell* **88** 511–21 (Condensin)
[54] Michaelis C, Ciosk R and Nasmyth K 1997 Cohesins: chromosomal proteins that prevent premature separation of sister chromatids *Cell* **91** 35–45
[55] Poirier M G and Marko J F 2002 Mitotic chromosomes are chromatin networks without a mechanically contiguous protein scaffold *Proc. Natl Acad. Sci.* **99** 15393–7
[56] Hirano T and Mitchison T J 1993 Topoisomerase ii does not play a scaffolding role in the organization of mitotic chromosomes assembled in xenopus egg extracts *J. Cell. Biol.* **120** 601–12
[57] Gerlich D, Hirota T, Koch B, Peters J-M and Ellenberg J 2006 Condensin I stabilizes chromosomes mechanically through a dynamic interaction in live cells *Curr. Biol.* **16** 333–44
[58] Hancock R 2007 Packing of the polynucleosome chain in interphase chromosomes: evidence for a contribution of crowding and entropic forces *Semin. Cell. Dev. Biol.* **18** 668–75 (review)
[59] Century T J, Fenichel I R and Horowitz S B 1970 The concentrations of water, sodium and potassium in the nucleus and cytoplasm of amphibian oocytes *J. Cell. Sci.* **7** 5–13
[60] Buravkov S V, Zierold K and Shakhlamov V A 1993 The mapping of the local content of water and dry matter by using ultrathin frozen sections *Bull. Eksp. Biol. Med.* **116** 325–8
[61] Päuser S, Zschunke A, Khuen A and Keller K 1995 Estimation of water content and water mobility in the nucleus and cytoplasm of xenopus laevis oocytes by nmr microscopy *Magn. Reson. Imaging* **13** 269–76
[62] Poirier M G, Monhait T and Marko J F 2002 Reversible hypercondensation and decondensation of mitotic chromosomes studied using combined chemical–micromechanical techniques *J. Cell. Biochem.* **85** 422–34
[63] Allen T D, Cronshaw J M, Bagley S, Kiseleva E and Goldberg M W 2000 The nuclear pore complex: mediator of translocation between nucleus and cytoplasm *J. Cell. Sci.* **113** 1651–9
[64] Paine P L, Moore L C and Horowitz S B 1975 Nuclear envelope permeability *Nature* **254** 109–14
[65] Hendzel M J, Wei Y, Mancini M A, Van Hooser A, Ranalli T, Brinkley B R, Bazett-Jones D P and Allis C D 1997 Mitosis-specific phosphorylation of histone h3 initiates primarily within pericentromeric heterochromatin during g2 and spreads in an ordered fashion coincident with mitotic chromosome condensation *Chromosoma* **106** 348–60
[66] Berger S L 2002 Histone modifications in transcriptional regulation *Curr. Opin. Genet. Dev.* **12** 142–8
[67] Zimmerman S and Minton A 1993 Macromolecular crowding: Biochemical, biophysical, and physiological consequences *Ann. Rev. Biophys. Bio.* **22** 27–65
[68] Asakura S and Oosawa F 1958 Interaction between particles suspended in solutions of macromolecules *J. Polym. Sci.* **33** 183–92
[69] de Gennes P G 1979 Suspensions colloidales dans une solution de polymeres *C. R. Acad. Sci.* **288** 359
[70] Odijk T 1996 Protein–macromolecule interactions *Macromolecules* **29** 1842–3
[71] Murphy L D and Zimmerman S 1995 Condensation and cohesion of lambda DNA in cell extracts and other media: implications for the structure and function of DNA in prokaryotes *Biophys. Chem.* **57** 71–92
[72] Verschure P J, van der Kraan I, Manders E M M, Hoogstraten D, Houtsmuller A B and van Driel R 2003 Condensed chromatin domains in the mammalian nucleus are accessible to large macromolecules *EMBO Rep.* **4** 861–6
[73] de Vries R 2006 Depletion-induced instability in protein–DNA mixtures: influence of protein charge and size *J. Chem. Phys.* **125** 014905
[74] Odijk T 1998 Osmotic compaction of supercoiled DNA into a bacterial nucleoid *Biophys. Chem.* **73** 23–9